Eur J Vasc Endovasc Surg **31**, 28–35 (2006)
doi:10.1016/j.ejvs.2005.07.018, available online at http://www.sciencedirect.com on SCIENCE DIRECT®

Embolization-driven Occlusion of the Abdominal Aortic Aneurysmal Sac as the Basis of Prevention of Endoleaks in a New Swine Model

P.H. Rolland,* V. Vidal, C. Mekkaoui, M.-F. Bertrand, O. Levrier and J.-M. Bartoli

Laboratory of Hemodynamics and Cardiovascular Mechanics, School of Medicine, La Timone Hospital for Adults, Mediterranean See University and Department of Radiology, Marseilles, France

Objectives. *To assess the effect of a new polymer in embolization of endoleaks using an animal model.*
Methods. *A modified aortic stent-graft was placed in 20 pigs. Embolization was performed at the time of graft insertion with non-cytotoxic* n*-butyl-2-cyanoacrylate-metacryloxysulpholane and lipiodol (0.2:0.8ratio, 2 ml). Angiography, scanning electron microscopy and immuno-histochemistry were obtained at day 0, 1 week and 3 months.*
Results. *In control animals both type I and II endoleaks were demonstrated. In treated animals, neither type-I nor type-II endoleaks were observed and a fibro-proliferative response was demonstrated within the aneurysm thrombus.*
Conclusions. *Host vascular responses govern the fate of the excluded aneurysm. Embolization of the sac and feeding arteries with non-cytotoxic glue sealed all occlusions by stimulating a massive restenosis-like process.*

Keywords: Porcine experimental models; Abdominal aortic aneurysm; Endovascular aneurysm repair; Endoleaks; Embolization; Aneurysm sac occlusion.

Introduction

Continued pressurization of the aortic sac following endovascular aneurysm repair (EVAR) of abdominal aortic aneurysm (AAA) has been associated with subsequent rupture.[1–8] Types I and II endoleaks are due to insufficient sealing at the graft ends or from retrograde collateral inflow via lumbar arteries and the inferior mesenteric artery (IMA).[8–11] Type I endoleaks are acknowledge to be dangerous, however, type II endoleaks have also been associated with aortic rupture and may facilitate the development of the former.[1–4,8,9,11–15] A number of approaches have been used in an attempt to embolize aortic branch vessels and prevent endoleak development.[4,16–23] One techniques is to inject liquid cyanoacrylate adhesives with anionic polymerisation, however, these agents appear to be toxic and damage the vascular intima.[24–26] Subsequent foreign-body responses can lead to vessel wall enlargement and neovascularization.[25,26] We previously reported the therapeutic efficacy of embolization of renal and brain arteries by using the standard *n*-butyl 2-cyanoacrylate monomers plus metacryloxysulpholane monomers, whose presence converts the polymerization pathway from an ionic to a radical mechanism which is a non-cytotoxic.[26] In this experimental study we investigate the non-cytotoxic embolization of the aortic aneurysm sac and feeding arteries following endo-grafting. We used an experimental porcine model creating by placing an endoluminal graft which occupied only around 50% of the aortic lumen leaving an external sac similar to endovascular repair of human AAA.

*Corresponding author. Pierre H. Rolland, PhD, LHMCV, School of Medicine, Mediterranean See University, 27, Bld Jean-Moulin, 13385 Marseille Cedex 5, France.
E-mail address: ph.rolland@medecine.univ-mrs.fr

Materials and Methods

Experimental protocol

The Ethics Committee granted approval for the present protocol. Twenty (controls, $n=8$; embolized, $n=12$) 5-months old, male Pietrin swines (45 ± 6 kg) (BlossinSA, Aubagne, France) were fed a standardized diet for pregnant sows to minimise weight gain (weight at 3 months 56 ± 7 kg).[19,26,27] Pigs were anesthetized with ketamine (15 mg/kg, IM) and midazolam (Hypnovel,

1078–5884/000028 + 08 $35.00/0

Roche, 0.5 mg, 10 ml^{-1} min^{-1}). Antibiotics (amoxicillin–clavulanic acid, 1 g:200 mg in 20 ml, IV) were given before and after the procedures.[27–30] The animals were euthanized with midazolam (50 mg in 10 ml), and chlorpromazine (25 mg) in 25 ml KCl 20% (w/v, bolus, IV).

Endoluminal aortic procedures

Stents, stent-grafts, delivery devices, and catheters were provided by Boston Scientific Corporation, Natick, USA. A custom made device incorporating a prosthesis (100×10 mm,Vanguard) and a Symphony nitinol stent (20×6 mm) placed inside a 12F introducer sheath (34 cm-long) was created.[20] A digital subtraction angiography system (GEMedical-System, Minneapolis,USA) was utilized for the procedures.[20,27] Percutaneous access was gained in both superficial femoral arteries (SFA) (11 cm 5F vascular sheaths). Pre- and post-procedure angiograms were obtained (Hexabrix, Guerbet Inc., 25 ml, 14 ml s^{-1}) via pigtail angiographic catheters (5F, 100 cm, tip with 1 cm-distant radiopaque markers) in the abdominal aorta. Dimensions and localization of the aorta and collaterals (renal and lumbar arteries) were computerized from the frames.[31] Via the left SFA, two Excelsior microcatheters (2.6F, 150 cm, 2.0F terminal part) were advanced into the mid (to deliver the embolisation material) and suprarenal aorta. The 5F sheath in right SFA was substituted for a 14 F introducer sheath and the stent-graft delivered to the infra-renal aorta. Pre-embolization angiograms of aorta and AAA sac (3 ml pure contrast-agent) were obtained. The microcatheter was connected to a 5-ml Luer-locked syringe (Medallion, Merit Medical, South Jordan, Utah) and flushed with isotonic 5% glucose solution. Glubran2 (GEM-Viareggio, Italy) glue was homogenized with ultrafluid lipiodol (Guerbet Lab, Aulnay/Bois, France) at 0.2:0.8 v/v proportions.[26] A 2 ml volume of the mixture was injected in a four-step procedure interspersed with flushing with isotonic glucose. Following digital haemostasis of the left SFA, and surgical closure of the right SFA, the animals were transferred to the post-operative holding room to recover. Further transcarotid angiograms were obtained 30 min post-procedure, day 7, and 3 months. In contrast to humans, pig spinal cord extends to the fifth lumbar vertebra. To prevent neurological events in the swine, the following pre- and post-implantation anticoagulant protocol was delivered: sodium heparin (10,000 IU in 1 ml, bolus) was given IV. before 6F–14F sheath replacement and after the embolization procedure; then, calcium-heparin (10,000 IU in 0.8 ml) was given subcutaneously, twice a day for 3 days, and finally the animals received calcium nadroparine (7600 IU antiXa in 0.8 ml) daily subcutaneously for a further 3 days.

Histology, scanning electron microscopy and morphometry

Following midline laparotomy, the stented segment from the abdominal aorta down to the iliacs arteries was sampled.[26–30] Specific attention was given to the lumbar arteries up to the backbone. Further catheterisation of the aorta was performed with a 22G intravenous catheter for repeated washings and perfusion with ph 7.3 buffered 10% formalin for fixation under a 120 mmHg pressure (15 min). Samples were fixed for 48 h, prior to being cut-open longitudinally

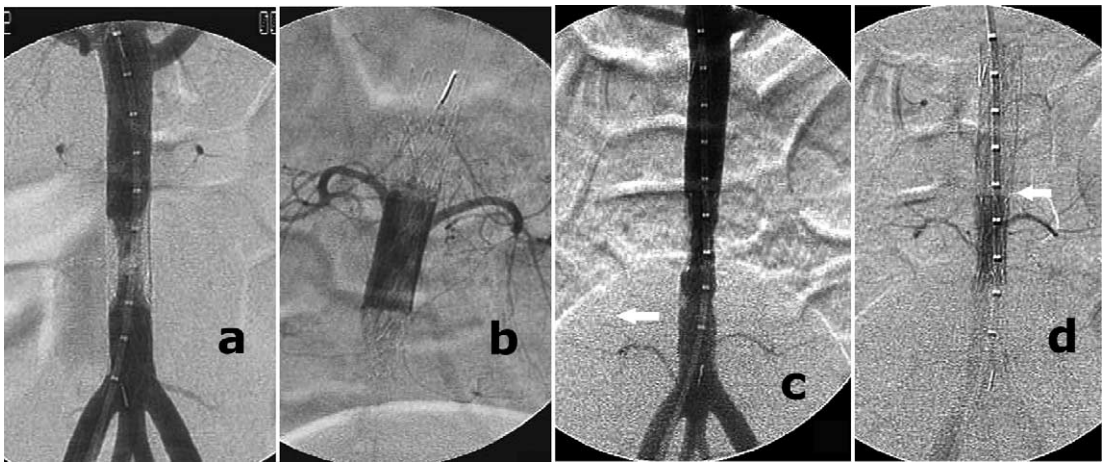

Fig. 1. Final intraoperative angiograms of the abdominal aorta, (a) showing reduction of the aortic lumen due to endoprosthesis placement (early angiographic phase); and of the aneurismal sac and lumbar arteries, (b) from microcatheter placed before endograft placement. At 3 months, anteroposterior aortogram shows the early-phase anterograde flow, (c) of lumbar arteries below the stent-graft and the late-phase retrograde, (d) lumbar flow to the aneurysm sac.

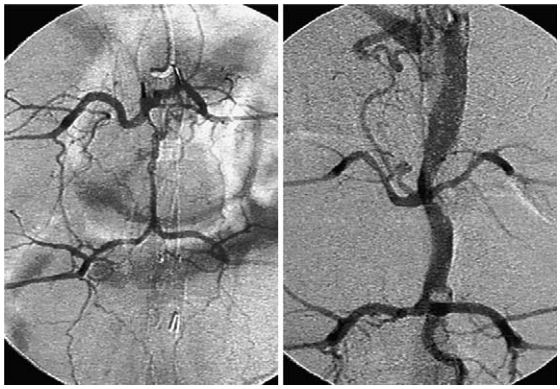

Fig. 2. Anteroposterior arteriograms obtained from selective positioning of the angiographic catheter tip above the upper neck of the endoprosthesis in control swines, at 3 months. A small right perigraft leakage demonstrated type II endoleak (left), the contrast media trace progressed in a retrograde manner from the patent lumbar branchs, to caudally feed the sac. The type I endoleak inflow (right) originated from the upper neck in the juxtarenal position, and it progressed ventrally to the proximal portion of the sac to feed the type II endoleak, and finally the egress of twisted type II endoleak was through both IMA and circulating lumbar arteries at the caudal endings of the sac. No distal type I endoleak was detected.

with a tungsten carbide scissors, with one half being processed for scanning electron microscopy (SEM), and second half for histology examination.[20,26,29–31] Longitudinally sectioned (5 μm) were cut from paraffin embedded samples. Samples for SEM examinations were either dehydrated in progressive alcohols or submitted to sputter coating with 30 nm gold prior to examination in the Quanta 200 SEM (FEI company, Eindhoven, The Netherlands) under low vacuum mode 1 Torr with water vapour.

Immunohistochemical staining for von Willbrand, FactorVIII and SMC-specific alpha-actin was performed on rehydrated deparafinized (5 μm) serial slides with appropriate blocking serum using rabbit or mouse monoclonal primary antibodies, and horseradish peroxidase or alkaline phosphatase enzymatic conjugates to the appropriate secondary antibodies with DAB or fast-red chromogen substrates.[28–31] When required, antigen retrieval using pepsin solution digests was carried out. All reagents were from Zymed Laboratories Inc (CA 94080, USA).

Results

Stent implantation and angiographic findings

The stent-grafts were placed with optimal immediate results in all cases, and no acute complications occurred during glue-lipiodol solution delivery. A single animal (control group) developed paraplegia on day 1 and died at day 8. Seven control (sacrificed at day 1, $n=1$, and 3 months, $n=6$) and twelve embolized (sacrificed at day 0, $n=3$, at week 1, $n=3$, and at 3 months, $n=6$) swines completed the study.

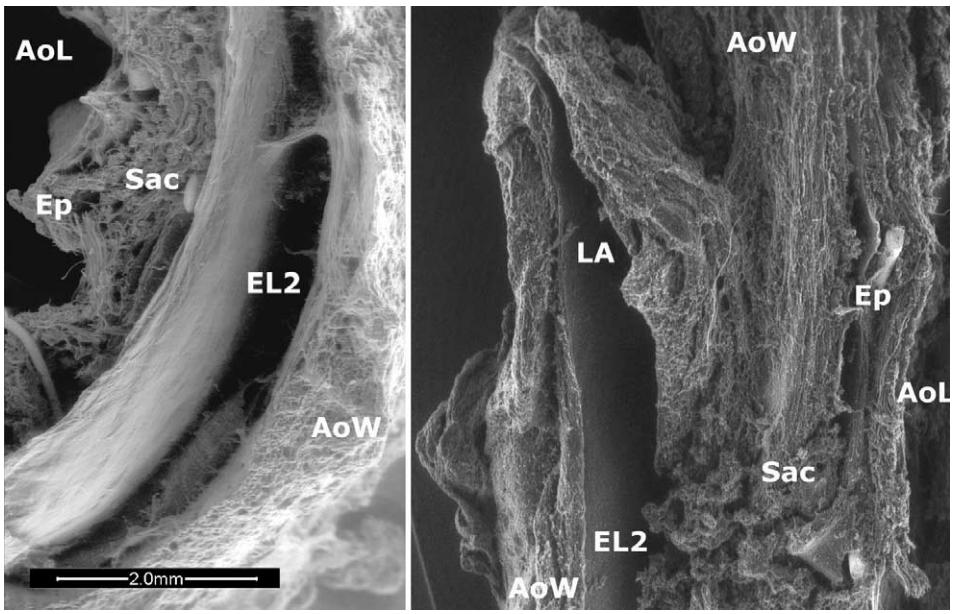

Fig. 3. Photographs from SEM investigations of transverse (left) and longitudinal (right) sections of the aneurysm sac in the graft-stented aorta in a control animal at 3 months. The patent aortic lumen (AoL) is separated from the aortic vascular wall (AoW) by the endoprosthesis (Ep), the type II endoleak (El2) and the aneurysm sac (sac). The endoleak was connected to the feeding lumbar artery (LA). The inner walls of the type II endoleak was covered by endothelial cells.

The mean pre- and post-procedure abdominal aortic diameter were 9.85±0.26 and 9.75±0.45 and 110.62±4.25 and 105.43±5.32 mm in length. The luminal constricted diameter of aorta was 5.88±0.54 and 5.53±0.42 mm pre and post stenting, respectively, (Fig. 1). At 3 months, the upper aortic neck was 9.98±0.35 and 10.15±0.29 mm in diameter in the grafted and graft-embolized groups. There was no significant difference in any of these diameters. No displacement of the grafts was noted by the end of the protocol. Late retrograde feeding of control AAA persisted via the lumbar arteries (Fig. 1).

The control aneurysm

At 3 months angiography demonstrated persistent type II endoleak in all control animals (Fig. 1). Three endoleaks were lateral to the aortic prosthesis (Fig. 2) and three were ventral. The endoleak channels were < 2 mm in diameter. Proximal type I endoleaks were demonstrated in two cases (Fig. 2). In each animal, outflow from the aneurysm was to the lumbar arteries and collaterals and in the two animals with type I endoleaks, the outflow path also involved the inferior mesenteric artery (Fig. 2). SEM in the control aneurysms at 3 months (Fig. 3) revealed the spatial organization of the type II leaks. Within organized thrombotic clots (fibrin fibers reinforced with collagen) and fibrocellular processes, the flow channel in the sac consisted of a thin, flat, free space with a curved shape paralleling the aneurysm crown concavity. The flow path passing through the organized thrombotic clots in the sac was lined by a monolayer of endothelial cells typical of neo-vascularisation.

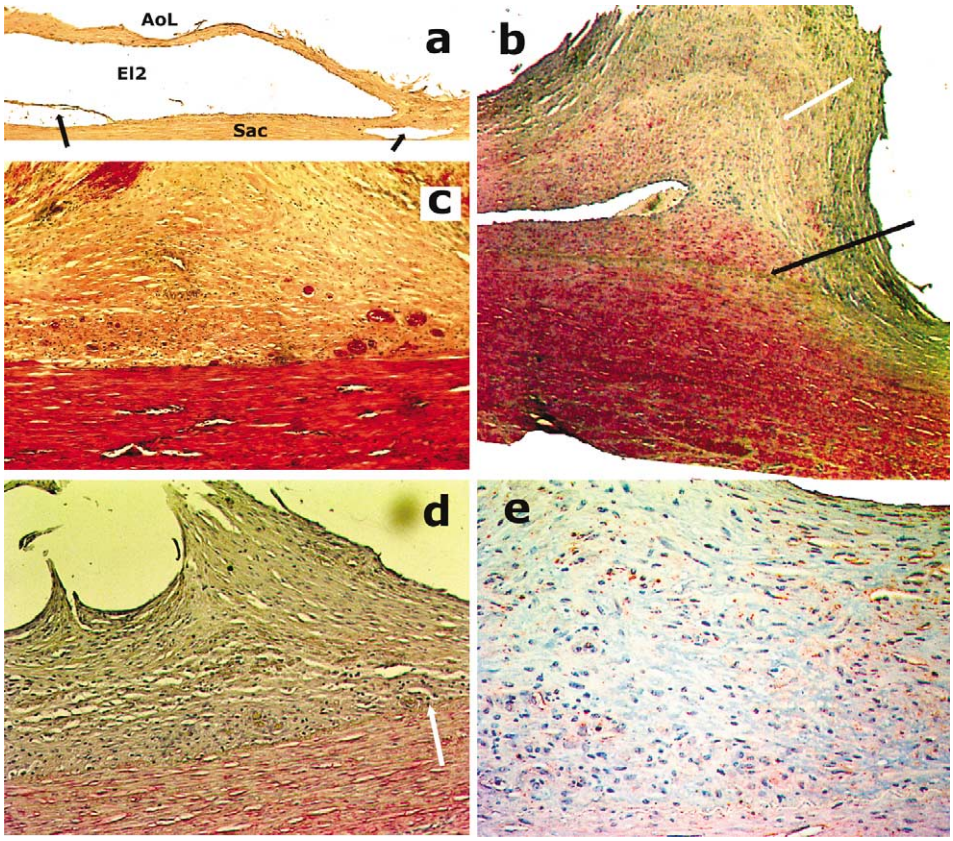

Fig. 4. Microphotographs of the aneurysm sac and aortic wall in control animals at 3 months, (a) the aneurysm sac materials embedded the type I endoleak (EI2) and secondary endothelial lined spaces (arrow), (b) fast-red immunohistochemistry of vascular smooth muscle (VSMC) alpha-actin in transverse sac-Aow section demonstrates that the sac was invaded by VSMC from AoW, as crossing of the internal elastic lamina (black arrow); and fibrocellular processes from myofibroblasts (white arrow) developed paralleling the sac contours, (c) HE-staining of the sac-AoW section shows small organized vessels with blood cells close to aortic intima and in AoW, (d) fast-red immunohistochemistry of vascular smooth muscle (VSMC) alpha-actin in transverse sac-Aow section further shows the absence of VSMC in the thrombotic materials; endothelial-cell lined lacunae emergence progressed in procession through the thrombotic materials from the intima of AoW (white arrow), (e) Horseradish peroxydase-based immunohistochemistry directed against FVIII-related antigens of endothelial cells demonstrates the endothelial nature of the cells underlining the lacunae within the sac thrombotic materials.

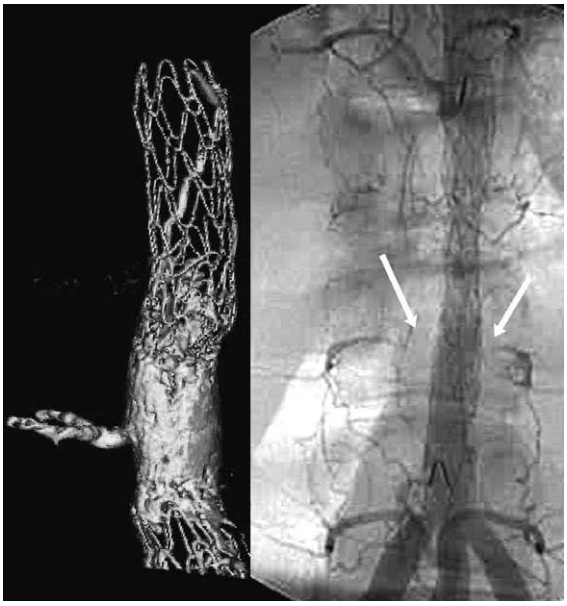

Fig. 5. 3D-reconstruction of embolized AAA at d0 (left). Aortic angiograms (right, late-phase) in animal with embolized aneurysm at 3 months show the persistent occlusion of embolized lumbar arteries (white arrows) despite the anterograde feeding of vicinal lumbar arteries.

Histology and immunohistochemistry observations further supported neo-vascularisation with endothelial-lined spaces of variable size from simple elementary lacunae to organized vessels containing red cells (Fig. 4). Smooth muscle cells (positive for alpha-actin) and myofibroblasts were present within the thrombus.

The embolized aneurysm

Complete embolization was achieved in each case by a four-step delivery of glue (2 ml final volume) within 225 ± 21 s. Typical tri-dimensional AAA reconstruction at day 0 and macroscopic appearance at 3 months are shown in Figs. 5 and 6, respectively. At 3 months, all grafted abdominal aorta were patent with no endoleaks (Fig. 5). Macroscopic examinations of longitudinally cut-opened abdominal aorta revealed that the non-embolized sac was entirely filled with only fresh thrombus at day 0, with both fresh and transformed thrombus at 1 week, and at 3 months there were substantial areas of solid fibrosclerotic material (Fig. 6). SEM in longitudinally cut-opened abdominal aorta (Fig. 7) showed that the glue polymerized slowly and hardened without fragmentation. The low reactivity and adhesive forces of the glue accounted for the presence of glue casts of the endoprosthesis and vascular walls without injuring either of them. At 1 week, the aneurysm was filled by the glue and organized fibrin deposits. At 3 months, the integrity of glue masses was preserved while the thrombus was replaced by a dense fibrocellular response. Histological examinations of the abdominal aorta, aneurysms sac and lumbar arteries in embolized animals confirmed the progressive fibrocellular response (Fig. 8). At day 0, the post-procedure occlusive process consisted of a plug made of the glue-lipiodol mixture embedding fresh thrombotic materials, sparsely attached to the intima, but without injuring the vascular wall (Fig. 8(A)). At 1 week,

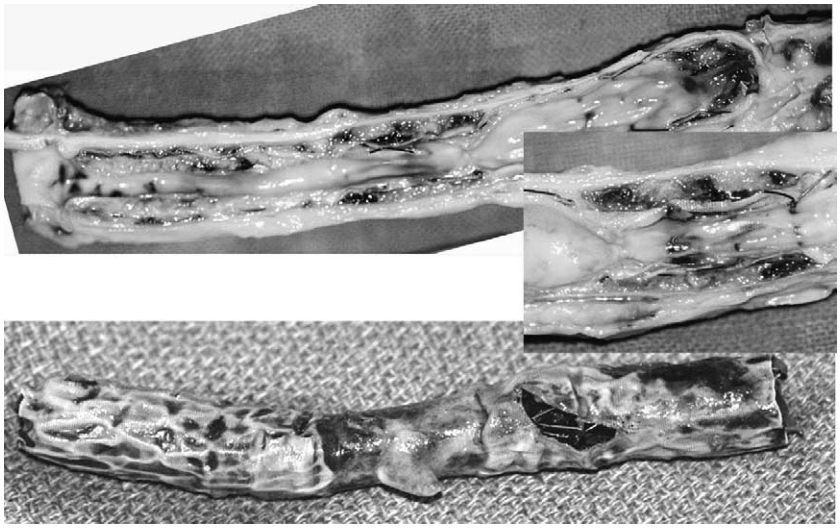

Fig. 6. Macroscopic appearances of the subrenal aorta at 3 months from a control, non-embolized animal (cut-opened artery, upper panel, right insert) showing the aneurysm, and from an embolized animal (closed prosthesis, lower panel) showing the whole mass of glue adhering to arterial wall up into the ostium of lumbar arteries.

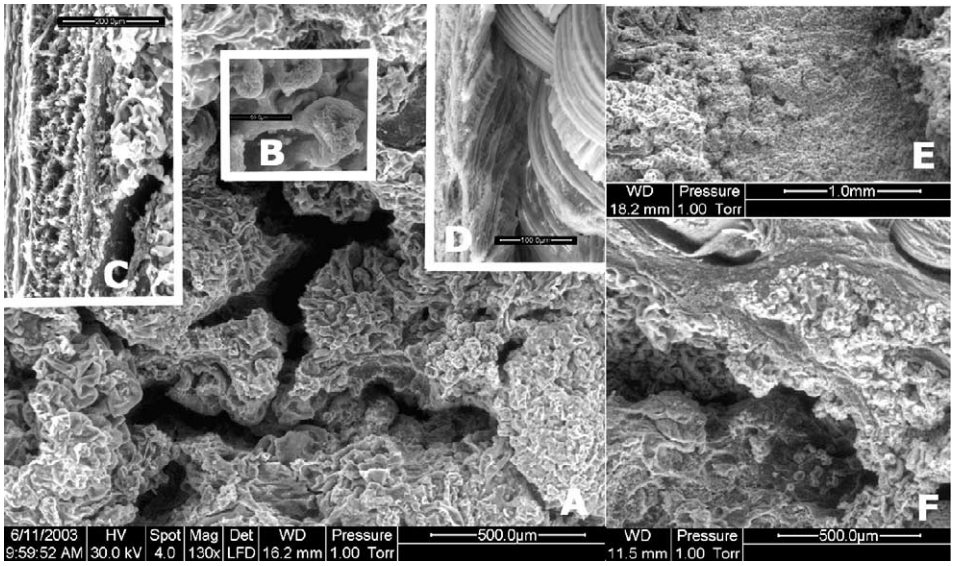

Fig. 7. Photographs from SEM investigations of the embolized AAA space show at day 0 budding of glue masses ((A) and (B)), closely adherent to vascular walls (C), with preservation of intima and internal elastic laminae, endoprosthesis cast (D), mixing of glue (left) and advanced thrombotic processes (right) at 1 week (E), and replacement of thrombotic clots by fibroproliferative materials, at 3 months (F).

the advanced thrombus, further converted to fibrils and clusters of fibrin, was embedded within the glue mass, and the arterial wall remained underlined by a thin fibrin film. The absence of fresh thrombus indicates that there was no longer blood circulation in the aneurysm and lumbar arteries (Fig. 8(B)). At 3 months, the luminal space was filled with a fibrocellular reaction due to proliferative myofibroblasts spreading from the arterial walls typical of restenosis (Fig. 8(C)).

Discussion

This study demonstrates that within a swine model of endografting the aneurysm sac thrombus undergoes a neo-vascular response which may support a type II endoleak. The type II endoleak may encourage the delayed development of a type I leak without proximal neck enlargement. The use of low toxicity glue was able to prevent endoleak development possibly by altering the type of repair response. A dense fibroproliferative response was evident in embolised arteries rather than the neo-vascular response seen in control animals.

The experimental model of aneurysm used was designed as a strictly catheter-based model in order to protect the infrarenal aorta and collaterals from iatrogenic surgical interventions, thereby enabling endoleak to be studied.[6,16–20] The limitation of this model is that the aneurysm did not increase in size over the mid-term, a process which may require a longer time to develop, provided weakening of the arterial wall actually occurs.[3,4,8,21,32]

The surprising development of proximal endoleak in two out of six animals at mid-term, was associated with maintained patency of the IMA and absence of sac thrombus.

We previously reported the efficacy of embolization of porcine renal and brain arteries by using a mixture of standard *n*-butyl-2-cyanoacrylate (nb-CA) monomers plus metacryloxysulpholane (MS) monomers whose presence converts the polymerization pathway from anionic to radical mechanisms.[26] The radically formed nb-CA casts poorly gripped and attached to the intima without injury, and finally embolized arteries presented without inflammatory crown surrounding the adventitia.[26] We report here that such non-cytotoxic embolization occurred in the aneurysm sac and the lumbar arteries by demonstrating that a polymerization mechanism independent of the reactive proteins in the vascular wall accounts for adherence of non-crystalline casts of prosthesis to the vessel walls. The non-cytotoxic embolization of the aneurysm sac and its feeding lumbar arteries drove aortic VSMCs and myofibroblasts to settle the transformed fibrin clots into fibrosclerotic structures embedding the glue masses. The concomitant resorption of lipiodol pockets by myofibroblasts enhanced the available luminal space for spreading processes. The aneurysm occlusion by proliferative SMCs and large amounts of collagen and proteoglycan-rich

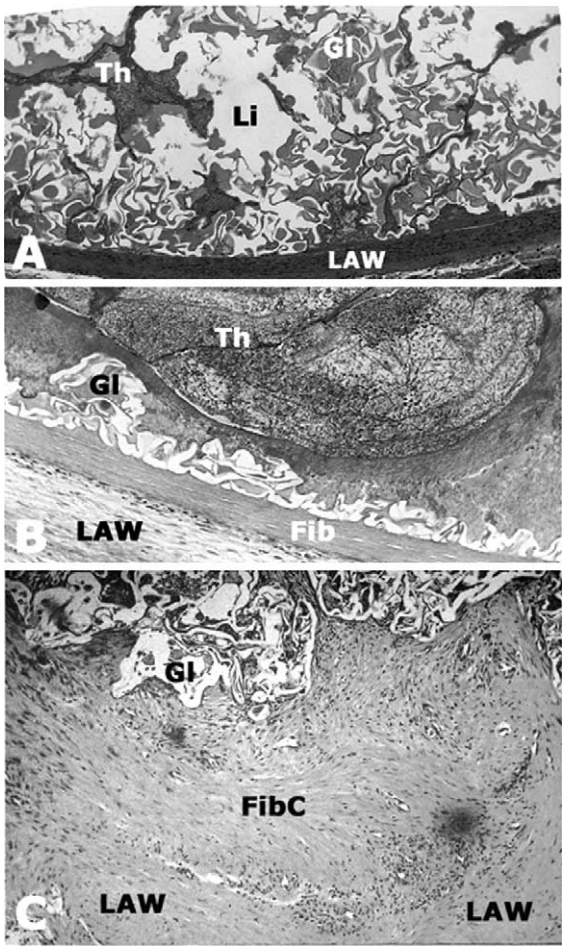

Fig. 8. Microphotographs of histopathologic changes in embolized lumbar arteries show the glue (Gl) masses embedding thrombotic pockets (Th) and voids previously filled with lipiodol (Li) in the absence of parietal injury (LAW: lumbar arterial walls), at day (0); and organized fibrino-sclerotic clots (Th) and fibrin (Fib) endothelial underlining of LAW at 1 week (B); and restenotic-like fibrocellular processes (FibC) colonizing the evanescent lumbar lumen and surrounding glue (Gl) masses at 3 months (C).

extra-cellular matrix develops to the detriment of the endothelial cell-mediated fibrinolysis and subsequent neovascularization observed in the patent aneurysm sac. One interesting pathological feature of the study is the findings that the fibrin clots in the embolized sac turned to transformed, stabilized fibrinosclerotic clots, whereas thrombus in the control sac retain the appearance of fresh thrombus made of non--transformed fibrin, at 3 months. The former condition was found to require myofibroblast spreading,[20] whereas persistence of leaks and endothelial cell-mediated fibrinolysis led to a continuous renewal of fibrin clots. Our findings support the development of techniques to inhibit neo-vascularisation of the thrombus within the aneurysm sac after EVAR. The clinical efficacy remains to be established.

References

1 Garcia-Madrid C, Josa M, Riambau V, Mestres CA, Muntana J, Mulet J. Endovascular *versus* open surgical repair of abdominal aortic aneurysm: a comparison of early and intermediate results in patients suitable for both techniques. *Eur J Vasc Endovasc Surg* 2004;**28**:365–372.

2 Criado FJ, Fairman RM, Becker GJ. Investigators talent LPS. Talent LPS AAA stent graft: results of a pivotal clinical trial. *J Vasc Surg* 2003;**37**:709–715.

3 Fan CM, Rafferty EA, Geller SC, Kaufman JA, Brewster DC, Cambria RP *et al*. Endovascular stent-graft in abdominal aortic aneurysms: the relationship between patent vessels that arise from the aneurysmal sac and early endoleak. *Radiology* 2001;**218**: 176–182.

4 Holtham SJ, Rose JDG, Jackson RW, Lees TA, Wyatt MG. The Vanguard endovascular stent-graft: mid-term results from a single centre. *Eur J Vasc Endovasc Surg* 2004;**27**:311–318.

5 Parodi JC, Berguer R, Ferreira LM, La Mura R, Schermerhorn ML. Intra-aneurysmal pressure after incomplete endovascular exclusion. *J Vasc Surg* 2001;**34**:909–914.

6 Hinnen JW, Visser MJT, van Bockel JH. Aneurysm sac pressure monitoring: effect of technique on interpretation of measurements. *Eur J Vasc Endovasc Surg* 2005;**29**:233–238.

7 Diaz S, Uzieblo MR, Desai KM, Talcott MR, Bae KT, Geraghty PJ *et al*. Type II endoleak in porcine model of abdominal aortic aneurysm. *J Vasc Surg* 2004;**40**:339–344.

8 Lin PH, Bush RL, Katzman JB, Zemel G, Puente OA, Katzen BT *et al*. Delayed aortic aneurysm enlargement due to endotension after endovascular abdominal aortic aneurysm repair. *J Vasc Surg* 2003;**38**:840–842.

9 Sampaio SM, Panneton JM, Mozes GI, Andrews JC, Bower TC, Karla M *et al*. Proximal type I endoleak after endovascular abdominal aortic aneurysm repair: predictive factors. *Ann Vasc Surg* 2004;**18**:621–628.

10 Chaudhuri A, Ansdell LE, Grass AJ, Adiseshiah M. Intrasac pressure waveforms after endovascular aneurysm repair (EVAR) are a reliable marker of type I endoleaks, but not type II or combined types: an experimental study. *Eur J Vasc Endovasc Surg* 2004;**28**:373–378.

11 Timaran CH, Ohki T, Rhee SJ, Veith FJ, Gargiulo NJ, Toriumi H *et al*. Predicting aneurysm enlargement in patients with persistent type II endoleaks. *J Vasc Surg* 2004;**39**:1157–1162.

12 Gorich J, Rilinger N, Sokiranski R, Orend KH, Ermis C, Kramer SC *et al*. Leakages after endovascular repair of aortic aneurysms: classification based on findings at CT, angiography, and radiography. *Radiology* 1999;**213**:767–772.

13 Stavropoulos SW, Baum RA. Catheter-based treatments of endoleaks. *Semin Vasc Surg* 2004;**17**:279–283.

14 Solis MM, Ayerdi J, Babcock GA, Parra JR, McLafferty RB, Gruneiro LA *et al*. Mechanism of failure in the treatment of type II endoleak with percutaneous coil embolization. *J Vasc Surg* 2002; **36**:485–490.

15 van Marrewijk CJ, Fransen G, Laheij RJF, Harris PL, Buth J. EUROSTAR C Is a type II endoleak after EVAR a harbinger of risk? Causes and outcome of open conversion and aneurysm rupture during follow-up. *Eur J Vasc Endovasc Surg* 2004;**27**:128–137.

16 Pavcnik D, Andrews RT, Yin Q, Uchida BT, Timmermans HA, Corless C *et al*. A canine model for studying endoleak after endovascular aneurysm repair. *J Vasc Interv Radiol* 2003;**1410**: 1303–1310.

17 Boudghene FP, Sapoval MR, Bonneau M, Leblanche AF, Lavaste FC, Michel JBL. Abdominal aortic aneurysms in

sheep—prevention of rupture with endoluminal stent-grafts. *Radiology* 1998;**206**:447–454.
18 Lerouge S, Raymond J, Salazkin I, Qin Z, Gaboury L, Cloutier G *et al*. Endovascular aortic aneurysm repair with stent-grafts: experimental models can reproduce endoleaks. *J Vasc Interv Radiol* 2004;**15**:971–979.
19 Raghavan ML, Vorp DA, Federle MP, Makaroun MS, Webster MW. Wall stress distribution on three-dimensionally reconstructed models of human abdominal aortic aneurysm. *J Vasc Surg* 2000;**31**:760–769.
20 Piquet P, Rolland PH, Bartoli JM, Tranier P, Moulin G, Mercier C. Tantalum-Dacron coknit stent for endovascular treatment of aortic aneurysms: a preliminary experimental study. *J Vasc Surg* 1994;**19**:698–706.
21 Baum RA, Stavropoulos SW, Fairman RM, Carpenter JP. Endoleaks after endovascular repair of abdominal aortic aneurysms. *J Vasc Interv Radiol* 2003;**14**:1111–1117.
22 Veith FJ, Baum RA, Ohki T, Amor M, Adiseshiah M, Blankensteijn JD *et al*. Nature and significance of endoleaks and endotension: summary of opinions expressed at an international conference. *J Vasc Surg* 2002;**35**:1029–1035.
23 Norwood MGA, Bown MJ, Lloyd G, Bell PRF, Sayers RD. The clinical value of the systemic inflammatory response syndrome (SIRS) in abdominal aortic aneurysm repair. *Eur J Vasc Endovasc Surg* 2004;**27**:292–298.
24 Pollak JS, White RI. The use of cyanoacrylate adhesives in peripheral embolization. *J Vasc Interv Radiol* 2001;**12**:907–913.
25 Gruber A, Mazal PR, Bavinzski G, Killer M, Budka H, Richling B. Repermeation of partially embolized cerebral arteriovenous malformations: a clinical, radiologic, and histologic study. *Am J Neuroradiol* 1996;**17**:1323–1331.
26 Levrier O, Mekkaoui C, Rolland PH, Murphy K, Cabrol P, Moulin G *et al*. Efficacy and low vascular toxicity of embolization with radical *versus* anionic polymerization of *n*-butyl-2-cyanoacrylate (NBCA)—An experimental study in the swine. *J Neuroradiol* 2003;**30**:95–102.
27 Rolland PH, Charifi AB, Verrier C, Bodard H, Friggi A, Piquet P *et al*. Hemodynamics and wall mechanics after stent placement in swine iliac arteries: comparative results from six stent designs. *Radiology* 1999;**213**:229–246.
28 Rolland PH, Bartoli JM, Piquet P, Mekkaoui C, Nott SH, Moulin G *et al*. Local delivery of NO-Donor molsidomine Post-PTA improves haemodynamics, wall mechanics and histomorphometry in atherosclerotic porcine SFA. *Eur J Vasc Endovasc Surg* 2002;**23**:226–233.
29 Rolland PH, Friggi A, Barlatier A, Piquet P, Latrille V, Faye MM *et al*. Hyperhomocysteinemia-induced vascular damage in the minipig. Captopril-hydrochlorothiazide combination prevents elastic alterations. *Circulation* 1995;**91**:1161–1174.
30 Rolland PH, Mekkaoui C, Vidal V, Berry JL, Moore JE, Moreno M *et al*. Compliance matching stent placement in the carotid artery of the Swine promotes optimal blood flow and attenuates restenosis. *Eur J Vasc Endovasc Surg* 2004;**28**:431–438.
31 Rolland PH, Mekkaoui C, Palassi M, Friggi A, Moulin G, Piquet P *et al*. Efficacy of local molsidomine delivery from a hydrogel-coated angioplasty balloon catheter in the atherosclerotic porcine model. *Cardiovasc Intervent Radiol* 2003;**26**:65–72.
32 Miskolczi L, Guterman LR, Flaherty LD, Hopkins LN. Saccular aneurysm induction by elastase digestion of the arterial wall: a new animal model. *Neurosurgery* 1998;**43**:595–600.

Accepted 7 July 2005
Available online 03 October 2005